

## Leaky wave radiation from planar anisotropic metamaterial slabs

Huikan Liu and Kevin J. Webb\*

*School of Electrical and Computer Engineering, Purdue University, 465 Northwestern Avenue, West Lafayette, Indiana 47907-2035, USA*  
(Received 30 December 2009; revised manuscript received 19 February 2010; published 14 May 2010)

We describe an optical leaky waveguide, which is achieved with uniaxially anisotropic metamaterials and can support both forward and backward leaky waves. The radiation behavior is analyzed with a transverse resonance approach, and supported by finite-element simulation results. The remarkable backward leaky nature can be exploited to develop a subdiffraction limit imaging system.

DOI: [10.1103/PhysRevB.81.201404](https://doi.org/10.1103/PhysRevB.81.201404)

PACS number(s): 78.67.Pt, 81.05.Xj, 42.25.Bs, 42.30.Va

Leaky wave antennas have been studied and used for many years due to their major advantages of high directivity and frequency scanning.<sup>1</sup> An ordinary dielectric slab with refractive index  $n > 1$  does not radiate effectively because most of the power is coupled into guided modes and trapped inside the slab. Therefore, the leaky modes are typically excited by introducing periodic scattering elements to excite fast-wave space harmonics.<sup>1</sup> To realize uniform leaky wave structures, potentially in the optical domain, a metamaterial slab with  $n \ll 1$  has been proposed to achieve a narrow radiation beam.<sup>2,3</sup> This approach suffers the limitation of large transverse slab dimensions because the operating wavelength inside the slab is much greater than the free-space wavelength, due to the small value of  $n$ . Also, low refractive index metamaterials that require small material permeabilities face implementation challenges.<sup>3,4</sup> In addition, the radiation only occurs in a narrow angular range between broadside and the critical angle,  $\sin^{-1}(n)$ , which limits beam scanning. Finally, we note that while a microstrip transmission line loaded with series capacitors and shunt inductors has been studied to realize metamaterial leaky wave antennas in the microwave frequency regime,<sup>5,6</sup> identifying the optical counterparts is difficult. To overcome these limitations, we present a uniform forward/backward radiating leaky waveguide at optical wavelengths based on uniaxially nonmagnetic anisotropic metamaterials having permittivity tensors in which one component is different from the others in sign.<sup>7</sup> The resulting hyperbolic dispersion relations under transverse magnetic (TM) excitation enable radiation from backfire ( $-90^\circ$ ) to endfire ( $90^\circ$ ), which is closely related to the positive and negative refraction characteristics of anisotropic media.<sup>8</sup> The slab thickness can be small relative to the free-space wavelength, and a metal-insulator stack can provide a convenient implementation.

To explore the leakage mechanism, we consider the anisotropic waveguide configuration of Fig. 1, where a TM wave ( $H_y, E_x, E_z$ ) travels in the  $+z$  direction with propagation constant  $k_z = \beta_z + i\alpha_z$ , determined by the physical parameters (material, geometry, and wavelength). The waveguide is illuminated by a magnetic line current source  $\mathbf{M}$ , which is located at  $x=0$  and oriented perpendicular to the  $x$ - $z$  plane, from the left at its edge. Such an arrangement will lead to a longitudinally asymmetrical radiation pattern. Consider, initially, that there is no material loss. The anisotropic slab is characterized by a dielectric tensor

$$\epsilon = \hat{x}\hat{x}\epsilon_x + (\hat{y}\hat{y} + \hat{z}\hat{z})\epsilon_z \quad (1)$$

with components satisfying the relation

$$\epsilon_x \epsilon_z < 0, \quad (2)$$

and the surrounding medium is assumed to be free space. By using the time convention  $\exp(-i\omega t)$ , and assuming no field variation in the  $y$  direction ( $k_y=0$ ), the TM fields in the anisotropic slab and surrounding free space have dispersion relations

$$k_x^2 \epsilon_z^{-1} + k_z^2 \epsilon_x^{-1} = k_0^2, \quad (3)$$

$$k_{0x}^2 + k_z^2 = k_0^2, \quad (4)$$

respectively, where  $k_0 = \omega \sqrt{\mu_0 \epsilon_0}$  is the free-space wave number. A transverse equivalent network in the  $x$  direction can be established to characterize the resonance condition,<sup>1</sup> giving the dispersion equation for TM modes supported by the structure. Referring to Fig. 1, the excitation generates all the even modes of the structure, in terms of  $H_y$ , and therefore the dispersion equation is

$$Z_0 - iZ \tan\left(\frac{k_x d}{2}\right) = 0, \quad (5)$$

where  $Z = k_x / \omega \epsilon_z \epsilon_0$  and  $Z_0 = k_{0x} / \omega \epsilon_0$  denote the characteristic impedances of the anisotropic slab and free space, respectively. Upon substitution of the impedances, the dispersion equation becomes

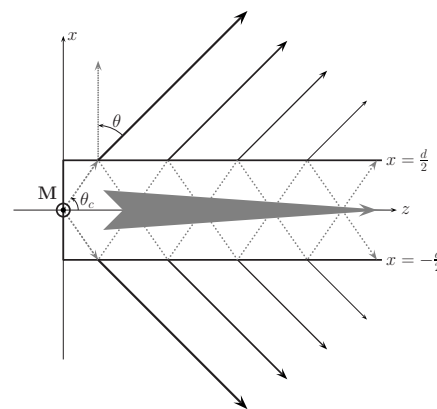


FIG. 1. Schematic representation of an anisotropic leaky wave structure. The gray dashed arrows inside the slab and the solid oblique arrows outside the slab denote the power flow in the waveguide and free space, respectively.

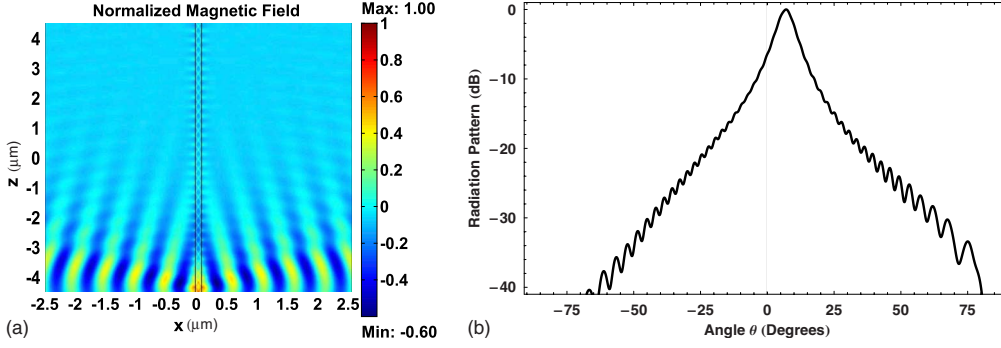


FIG. 2. (Color online) Forward anisotropic leaky waveguide,  $\epsilon_x = 0.01$ ,  $\epsilon_z = -0.1$ , the width of the slab is  $0.1 \mu\text{m}$  and  $\lambda = 0.5 \mu\text{m}$ . A filamentary magnetic current line source is located at  $(x=0, z=-4.5 \mu\text{m})$ . (a) Full-wave (finite-element method) simulated real part of the  $H$ -field distribution. (b) The radiation pattern of the anisotropic waveguide, showing a principal peak located at  $\theta \approx 7.07^\circ$ .

$$\cos\left(\frac{k_x d}{2}\right) - \frac{ik_x}{\epsilon_z k_{0x}} \sin\left(\frac{k_x d}{2}\right) = 0. \quad (6)$$

Equation (6), with Eqs. (3) and (4), is an eigenvalue equation in  $k_z$ . The case  $k_z = \beta_z > k_0$  corresponds to modes with phase constant  $\beta_z$  guided by the slab, whereas for a leaky wave,  $k_z = \beta_z + i\alpha_z$  is complex, with leakage rate  $\alpha_z > 0$ .<sup>1</sup> It follows from Eq. (4) that  $k_{0x}$  is also complex, i.e.,  $k_{0x} = \beta_{0x} + i\alpha_{0x}$ , with  $\beta_{0x} > 0$ , and forming the real and imaginary parts of Eq. (4) yields

$$\beta_{0x}\alpha_{0x} + \beta_z\alpha_z = 0, \quad (7)$$

$$\beta_z^2 - \alpha_z^2 + \beta_{0x}^2 - \alpha_{0x}^2 = k_0^2. \quad (8)$$

From Eq. (7), we can determine the sign of  $\alpha_{0x}$  based on the sign of  $\beta_z$ , given that we must have  $\alpha_z > 0$ : if  $\beta_z > 0$ ,  $\alpha_{0x} < 0$  (improper wave), and if  $\beta_z < 0$ ,  $\alpha_{0x} > 0$  (proper wave). From Eq. (8), we thus have the condition on  $\beta_z$  for leakage as

$$\beta_z^2 < k_0^2 + \alpha_z^2 + \alpha_{0x}^2. \quad (9)$$

For many leaky wave antenna applications, we are interested in finding possible solutions of Eq. (6) offering large effective radiation aperture and resulting narrow beamwidth (high gain). We thus require low values of  $\alpha_z$ , which from Eq. (9) results in

$$\alpha_z \ll k_0, \quad -k_0 < \beta_z < k_0. \quad (10)$$

The radiation occurs under the angle  $\theta = \sin^{-1}(\beta_z/k_0)$  with respect to the broadside direction (the  $x$  direction). Numerical analysis reveals that solutions of Eq. (6) subject to the conditions in Eq. (10) exist, and a mathematically sufficient condition of the dielectric tensor for leakage into free space is that  $|\epsilon_x| \ll 1$ , which is a salient sign of anisotropic  $\epsilon$ -near-zero metamaterials.<sup>9</sup> For the case that  $|\epsilon_x| \ll 1$ , from Eq. (3)

$$k_z = \sqrt{\epsilon_x k_0^2 - \epsilon_x k_x^2 / \epsilon_z} \approx \pm \sqrt{-\epsilon_x / \epsilon_z} k_x, \quad (11)$$

where the sign on the right-hand side is determined by adding perturbational loss and enforcing  $\alpha_z > 0$ , and depends on the signs of  $\epsilon_x$  and  $\epsilon_z$ , that is, “+” is assumed if  $\epsilon_x > 0$  and  $\epsilon_z < 0$  whereas  $\epsilon_x < 0$  and  $\epsilon_z > 0$  leads to “-” (Ref. 10). Given appropriate values of  $k_x$ ,  $k_z$  can be specified to satisfy the condition in Eq. (10). As suggested by Eq. (11), the power flow extending outward from the source inside the slab forms a resonance cone,<sup>11,12</sup> where the half angle of the cone is defined as  $\theta_c = \arctan \sqrt{-\epsilon_x / \epsilon_z}$ , and the resulting highly confined beams travel in a raylike manner with each “bounce

off” at the waveguide boundaries accompanied by a certain portion of power leakage, which is schematically illustrated in Fig. 1.

Depending on the signs of  $\epsilon_x$  and  $\epsilon_z$ , the leaky waveguide can exhibit right-handed ( $\beta_z > 0$ ) or left-handed ( $\beta_z < 0$ ) behavior. If  $\epsilon_x > 0$  and  $\epsilon_z < 0$ , the structure operates in right-handed mode because from Eq. (11),  $\beta_z > 0$ , and the improper wave propagates forward. If  $\epsilon_x < 0$  and  $\epsilon_z > 0$ , the structure operates in left-handed mode because  $\beta_z < 0$ , and the proper wave propagates backward. The forward/backward propagation characteristics are direct consequences of the right/left handedness of strongly anisotropic media.<sup>8,13</sup> The desired anisotropy,  $\epsilon_x \epsilon_z < 0$ , can be accomplished at infrared and visible frequencies with periodic composite structures, for example, multilayer metal-insulator stacks<sup>8,11,14</sup> or nanowire media,<sup>13</sup> provided the periodicity is much smaller than the operating wavelength. We note that the anisotropic metamaterial leaky waveguide does not require periodic scattering elements for achieving leakage, making it fundamentally different from the usual leaky wave antenna.<sup>1</sup>

In Figs. 2 and 3, we investigate the field distribution and radiation patterns of forward and backward leaky waveguides having subwavelength slab thickness ( $\lambda/5$ , with  $\lambda$  the free-space wavelength), with the physical parameters (wavelength, dielectric tensor, and slab width) chosen such that there is one dominant leaky mode. In Fig. 2, the dominant mode has  $k_z/k_0 = 0.12 + i0.065$ , by solving Eq. (6), leading to the radiation angle  $\theta = 7.0^\circ$ . The finite-element simulation results obtained using the commercial software package COMSOL (Ref. 15) show the distribution of the real part of magnetic field in Fig. 2(a) and the radiation pattern in Fig. 2(b). The simulated angle of the maximum of the beam agrees well with the theoretical prediction. In Fig. 3, the dominant mode is given by  $k_z/k_0 = -0.91 + i0.0074$ , and consequently the beam angle is  $\theta = -65.2^\circ$ , which is consistent with the full-wave simulation result Fig. 3(b).

One way to demonstrate an optical leaky waveguide with anisotropic metamaterials, based on use of a metal-insulator stack, and to enhance the local leakage, is to embed the slab in a dielectric host with large dielectric constant  $\epsilon_r$ . In contrast to Eq. (10), the leakage into the dielectric host then occurs for

$$\alpha_z \ll \sqrt{\epsilon_r} k_0, \quad -\sqrt{\epsilon_r} k_0 < \beta_z < \sqrt{\epsilon_r} k_0, \quad (12)$$

and  $|\epsilon_x| \ll \sqrt{\epsilon_r}$  can secure the existence of leaky wave solutions. In Fig. 4, we investigate the homogenized Ag/SiO<sub>2</sub>

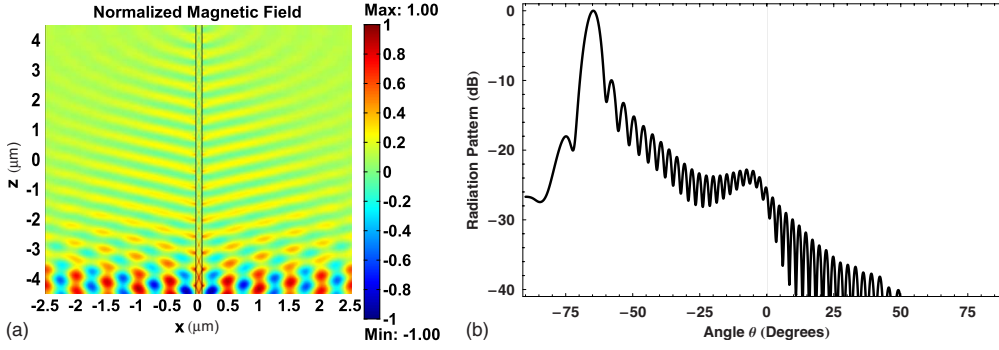


FIG. 3. (Color online) Backward anisotropic leaky waveguide,  $\epsilon_x = -0.01$ ,  $\epsilon_z = 0.3$ , the width of the slab is  $0.1 \mu\text{m}$  and  $\lambda = 0.5 \mu\text{m}$ . (a) Full-wave simulated real part of the  $H$ -field distribution. (b) The radiation pattern of the anisotropic waveguide, showing a principal peak located at  $\theta \approx -65.46^\circ$ .

metal-insulator stack embedded in a Si host as a possible realization of an anisotropic leaky waveguide. The homogenized uniaxial dielectric tensor components  $\epsilon_{\parallel}$  and  $\epsilon_{\perp}$ , parallel and perpendicular to the stack surface, are given by  $\epsilon_{\parallel} = D\epsilon_{\text{Ag}} + (1-D)\epsilon_{\text{SiO}_2}$  and  $\epsilon_{\perp} = [D/\epsilon_{\text{Ag}} + (1-D)/\epsilon_{\text{SiO}_2}]^{-1}$ , where  $D$  is the volume fraction occupied by Ag, and the orientation of the stack is defined so that  $\epsilon_x = \epsilon_{\parallel}$ ,  $\epsilon_z = \epsilon_{\perp}$ . The finite-element simulation results for the field distributions, as shown in Fig. 4, clearly demonstrate that for particular wavelengths, the slab behaves as an optical leaky waveguide radiating forward or backward, due to the signs of the effective  $\epsilon_x$  and  $\epsilon_z$  [ $\text{Re}(\epsilon_x) < 0$  and  $\text{Re}(\epsilon_z) > 0$  leads to backward radiation]. More specifically, by solving the modified version of Eq. (6) that incorporates  $\epsilon_r$  of the surrounding medium, the dominant  $k_z$  is obtained as  $k_z/k_0 = 0.63 + i0.18$  for Fig. 4(a),  $k_z/k_0 = -3.40 + i0.45$  for Fig. 4(b), and  $k_z/k_0 = -3.00 + i0.329$  for Fig. 4(c). The magnetic current source for generating leaky waves, as shown in Fig. 4, can be practically implemented by impinging a plane wave on a screen (made from Cr) with a narrow aperture. Although leakage has been noted from a right-handed leaky waveguide composed of an anisotropic metamaterial achieved with a semiconductor stack,<sup>17</sup> we identify the existence of left-handed leaky modes and characterize possible solutions using a transverse resonance analysis.

A planar near-field subdiffraction limit imaging system can be envisioned by pairing a backward leaky waveguide with a Si slab, as shown in Fig. 5. The waves radiated from

the source emerge as strongly confined beams inside the anisotropic slab, with the direction defined by the resonance cone angle  $\theta_c$ , and then reradiate into the backward quadrant at the interface between the anisotropic waveguide and the Si slab to form a focal point at a certain distance from the interface. The physical mechanism is illustrated in Fig. 5(a), obtained with a full-wave finite-element simulation. Because the leaky mode supported by the system can have a subwavelength transverse propagation constant,  $|\text{Re}(k_z)| > k_0$  [cf. Fig. 4(b), where  $k_z/k_0 = -3.40 + i0.45$ ], it enables the transfer of subdiffraction limit features to the image plane. Figures 5(b) and 5(c) show the normalized amplitudes of the magnetic and electric fields at the image plane. In Fig. 5(b), the field amplitudes in the image plane are compared with the diffraction limit for a current line source from a continuous spectrum without the lens, given by<sup>18</sup>

$$C \int_{-k_0}^{k_0} \frac{e^{ik_z z}}{\sqrt{k_0^2 - k_z^2}} dk_z = C J_0(k_0 z), \quad (13)$$

where  $J_0(\cdot)$  is the Bessel function of the first kind, of order zero, and  $C$  is a normalizing constant. Because the distance from the object to the image plane is large, the diffraction-limited pattern  $C J_0(k_0 z)$  does not contain contributions from the evanescent fields. Despite the resemblance between the present imaging system and the bilayer lens, which uses two bulk media with opposite handedness for negative refraction,<sup>7,10</sup> the fundamental difference is that the bilayer

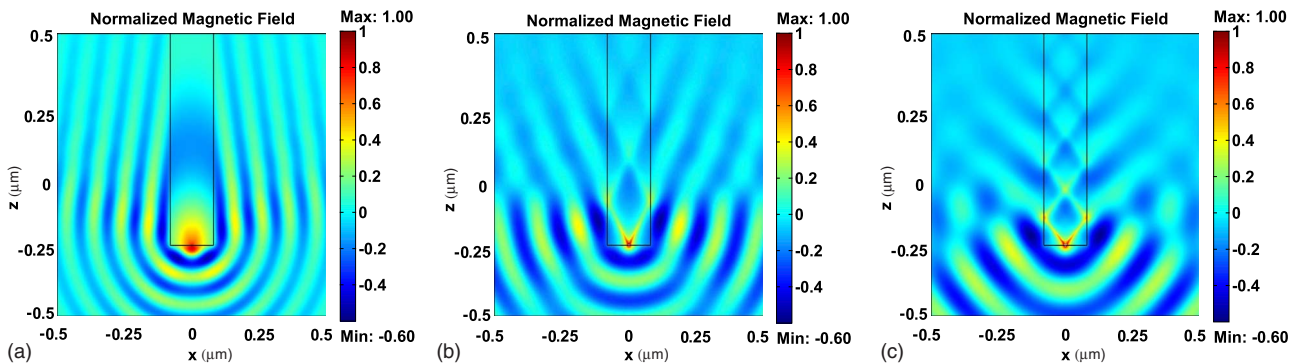


FIG. 4. (Color online) Full-wave simulated real part of the  $H$ -field distribution of a Ag/SiO<sub>2</sub> bulk anisotropic leaky waveguide embedded in a Si host. The volume fraction for Ag is  $D = 0.2$ . The width of the slab is  $0.16 \mu\text{m}$ . A magnetic current line source is located at ( $x = 0$ ,  $z = -0.25 \mu\text{m}$ ). (a)  $\lambda = 459.2 \text{ nm}$ ,  $\epsilon_{\text{Si}} = 20.99 + i1.19$ ,  $\epsilon_{\text{Ag}} = -6.53 + i0.74$ , and  $\epsilon_{\text{SiO}_2} = 2.14$  (Ref. 16), giving rise to  $\epsilon_x = 0.41 + i0.15$  and  $\epsilon_z = 2.91 + i0.029$ . (b)  $\lambda = 563.6 \text{ nm}$ ,  $\epsilon_{\text{Si}} = 16.3 + i0.26$ ,  $\epsilon_{\text{Ag}} = -11.89 + i0.83$ , and  $\epsilon_{\text{SiO}_2} = 2.13$ , giving  $\epsilon_x = -0.67 + i0.17$  and  $\epsilon_z = 2.79 + i9.05 \times 10^{-3}$ . (c)  $\lambda = 652.6 \text{ nm}$ ,  $\epsilon_{\text{Si}} = 14.8 + i0.123$ ,  $\epsilon_{\text{Ag}} = -17.2 + i1.16$ , and  $\epsilon_{\text{SiO}_2} = 2.12$ , giving  $\epsilon_x = -1.74 + i0.23$  and  $\epsilon_z = 2.74 + i5.85 \times 10^{-3}$ .

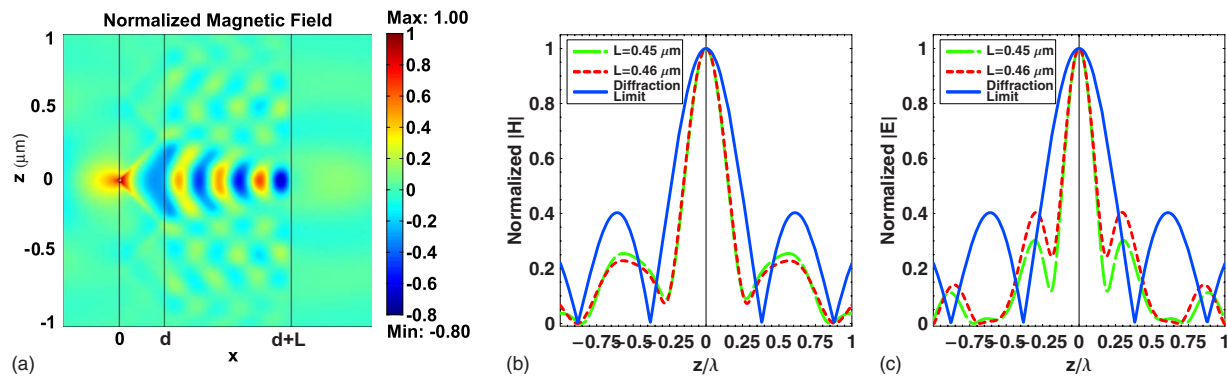


FIG. 5. (Color online) Finite-element simulation of a Ag/SiO<sub>2</sub> bulk anisotropic leaky waveguide juxtaposed with a Si slab, functioning as a subdiffraction imaging system. The operating wavelength is  $\lambda=563.6$  nm, and the material parameters are specified in Fig. 4. The thickness of the waveguide is  $d=0.16$   $\mu\text{m}$ , the thickness of silicon slab is  $L$ , and the surrounding medium is assumed to be free space. The excitation current line source is located at the left exit face of the waveguide. (a) Real part of the magnetic field plot  $H_y(x,z)$  for  $L=0.45$   $\mu\text{m}$ . (b) The magnetic field profile at the image plane (the right interface of the silicon slab). (c) The electric field profile at the image plane.

lens preserves subwavelength information through continuous spectra whereas the present system employs only a discrete number of leaky modes to accomplish resolution enhancement, and the seemingly negative refraction at the interface between the anisotropic slab and the isotropic slab is in essence a backward leakage. One compelling advantage of the imaging system in Fig. 5(a) over conventional subwavelength lenses is that it does not impose any restrictions on impedance match or operating wavelength, as long as it operates in backward leaky wave mode. Another advantage is that it requires the synthesis of only one anisotropic bulk medium. The imaging performance, according to Figs. 5(b) and 5(c), is robust to small variations in the thickness of the isotropic slab  $L$ . Also, the resolution of this imaging system, similar to immersion microscopes,<sup>19</sup> is inherently limited by  $\sim\lambda/2n_{\text{Si}}$ , because field components with  $k_z > n_{\text{Si}}k_0$  are exponentially decaying in the Si layer. One important difference of this imaging system from the immersion microscope,

however, is that the Si layer acts as a focusing agent rather than an immersion media for collecting light. Reference 8 suggests an imaging scheme based on anisotropic waveguide modes. The fundamental difference is that Ref. 8 considers slow waves (or guided waves) while our system exploits fast waves (or leaky waves).

In conclusion, we propose a class of optical forward/backward radiating leaky waveguides based on uniaxially anisotropic metamaterials. The quantitative behavior is analytically characterized and verified by numerical simulation results. As one application, we show an imaging system with a resolution beyond the diffraction limit by exploiting the backward radiating nature of the leaky waveguide. The notion should find important applications in optical nanoantennas.

This work was supported by the National Science Foundation (Grants No. 0524442 and No. 0901383) and the Department of Energy (Grant No. DE-FG52-06NA27505).

\*webb@purdue.edu

<sup>1</sup>A. A. Oliner and D. R. Jackson, in *Antenna Engineering Handbook*, 4th ed., edited by J. L. Volakis (McGraw-Hill, New York, 2007).

<sup>2</sup>S. Enoch, G. Tayeb, P. Sabouroux, N. Guérin, and P. Vincent, *Phys. Rev. Lett.* **89**, 213902 (2002).

<sup>3</sup>P. Baccarelli, P. Burghignoli, F. Frezza, A. Galli, P. Lampariello, G. Lovat, and S. Paulotto, *IEEE Trans. Microwave Theory Tech.* **53**, 32 (2005).

<sup>4</sup>A. Alù, F. Bilotti, N. Engheta, and L. Vegni, *IEEE Trans. Antennas Propag.* **54**, 1632 (2006).

<sup>5</sup>S. Lim, C. Caloz, and T. Itoh, *IEEE Trans. Microwave Theory Tech.* **52**, 2678 (2004).

<sup>6</sup>C. Caloz and T. Itoh, *Electromagnetic Metamaterials: Transmission Line Theory and Microwave Applications* (Wiley, New York, 2005).

<sup>7</sup>D. R. Smith and D. Schurig, *Phys. Rev. Lett.* **90**, 077405 (2003).

<sup>8</sup>L. V. Alekseyev and E. Narimanov, *Opt. Express* **14**, 11184 (2006).

<sup>9</sup>N. Engheta, *Science* **317**, 1698 (2007).

<sup>10</sup>H. Liu, Shivanand, and K. J. Webb, *Opt. Lett.* **34**, 2243 (2009).

<sup>11</sup>B. Wood, J. B. Pendry, and D. P. Tsai, *Phys. Rev. B* **74**, 115116 (2006).

<sup>12</sup>J. K. H. Wong, K. G. Balmain, and G. V. Eleftheriades, *IEEE Trans. Antennas Propag.* **54**, 2742 (2006).

<sup>13</sup>V. A. Podolskiy and E. E. Narimanov, *Phys. Rev. B* **71**, 201101(R) (2005).

<sup>14</sup>K. J. Webb and M. Yang, *Opt. Lett.* **31**, 2130 (2006).

<sup>15</sup><http://www.comsol.com/products/>

<sup>16</sup>*Handbook of Optical Constants of Solids*, edited by E. D. Palik (Academic Press, New York, 1998).

<sup>17</sup>A. J. Hoffman, V. A. Podolskiy, D. L. Sivco, and C. Gmachl, *Opt. Express* **16**, 16404 (2008).

<sup>18</sup>J. Zhu and G. V. Eleftheriades, *Phys. Rev. Lett.* **101**, 013902 (2008).

<sup>19</sup>R. R. Kingslake, *Optical System Design* (Academic Press, London, 1983).